

$\pi^+$  photoproduction from  $^{13}\text{C}$

J. LeRose,\* K. Min, D. Rowley,<sup>†</sup> B. O. Sapp, P. Stoler, P.-K. Teng, E. J. Winhold, and P. F. Yergin  
 Department of Physics, Rensselaer Polytechnic Institute, Troy, New York 12181

A. M. Bernstein, K. I. Blomqvist, H. S. Caplan,<sup>‡</sup> S. A. Dytman, G. Franklin,<sup>§</sup> and M. Pauli<sup>||</sup>  
 Laboratory for Nuclear Science, Massachusetts Institute of Technology, Cambridge, Massachusetts 02139

K. Shoda and M. Yamazaki

Laboratory of Nuclear Science, Tohoku University, Mikamine, Sendai 982, Japan

(Received 22 April 1982)

Differential cross section measurements were made for  $^{13}\text{C}(\gamma, \pi^+)^{13}\text{B}(\text{g.s.})$  at  $90^\circ$  (lab) for pion energies of 18, 29, and 42 MeV, and for  $^{13}\text{C}(\gamma, \pi^+)^{13}\text{B}$  ( $E_x=3.5$  MeV) at 42 MeV. The ground-state results are compared to several distorted-wave impulse approximation calculations and to Helm model calculations. There are significant discrepancies between experiment and theory and among the theoretical results.

[ NUCLEAR REACTIONS  $^{13}\text{C}(\gamma, \pi^+)^{13}\text{B}$  ( $E_x=0, 3.5$  MeV),  $\theta_\pi=90^\circ$  (lab),  $E_\pi=18, 29, 42$  MeV, measured  $d\sigma/d\Omega$ , compared with DWIA calculations. ]

I. INTRODUCTION

Several experimental measurements of  $(\gamma, \pi^\pm)$  differential cross sections to discrete final states in light nuclei at pion energies below 50 MeV, where the pion-nucleus interaction is weak, have recently been reported by groups working at the MIT-Bates Linac and at Tohoku University. Cases studied include  $^{12}\text{C}(\gamma, \pi^\pm)$ ,<sup>1-3</sup>  $^{10}\text{B}(\gamma, \pi^\pm)$ ,<sup>4,5</sup>  $^{16}\text{O}(\gamma, \pi^+)$ ,<sup>6</sup>  $^9\text{Be}(\gamma, \pi^+)$ ,<sup>6,7</sup> and  $^6\text{Li}(\gamma, \pi^+)$ .<sup>8</sup> This recent growth in experimental data has inspired a number of calculations based on the distorted wave impulse approximation (DWIA). Presently the emphasis of the field is on studies of the reaction mechanism in cases where the nuclear structure is fairly well understood. The agreement between experiment and theory for the cases listed above is somewhat mixed, though in most cases it is better than a factor of 2. The recent experimental results<sup>4</sup> on the  $^{10}\text{B}(\gamma, \pi)$  ground-state transition are surprising since there is poor agreement with several DWIA calculations just where one expects the theory to work relatively well (a pure  $M3$  transition whose form factor is well known and expected to be predominantly spin-flip).

The  $^{13}\text{C}(\gamma, \pi^+)^{13}\text{B}(\text{g.s.})$  reaction studied in the present experiment should be an additional good test case since the transition to the 15.11 MeV  $\frac{3}{2}^-$

state in  $^{13}\text{C}$ , which is the analog of the  $^{13}\text{B}$  ground state (see Fig. 1), has been well studied in  $^{13}\text{C}(e, e')$ .<sup>9-11</sup> Moreover, the present work corresponds to a momentum transfer near  $q=1$  fm<sup>-1</sup>, where the form factor is relatively flat and near its maximum. The ground state transition can be readily resolved since the first excited state in  $^{13}\text{B}$  is

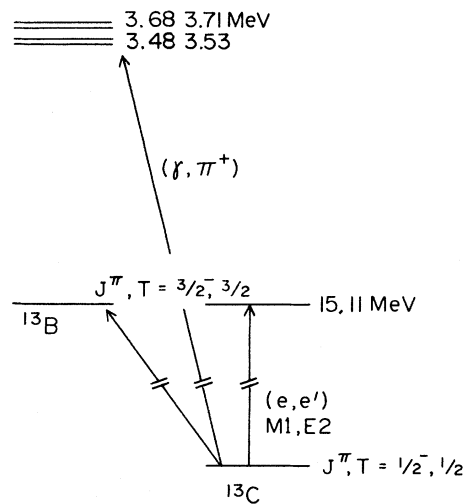


FIG. 1.  $A=13$  energy levels relevant for the present experiment (Ref. 38).

at 3.48 MeV. The present work studies  $\pi^+$  emission at  $90^\circ$  (lab) for pion energies of about 18, 29, and 42 MeV. Studies of  $^{13}\text{C}(\gamma, \pi^-)^{13}\text{N}(\text{g.s.})$  were also done and have been reported previously.<sup>12</sup> Angular distribution measurements on  $^{13}\text{C}(\gamma, \pi^+)^{13}\text{B}(\text{g.s.})$  at  $T_\pi = 40$  MeV were made at Tohoku University at the same time as the present experiment by a Tohoku-RPI-MIT collaboration.<sup>13</sup>

## II. EXPERIMENT

The experimental arrangement was similar to that used in earlier experiments done at Bates on  $^{12}\text{C}$  (Ref. 2) and  $^{10}\text{B}$ .<sup>4</sup> The layout is shown in Fig. 2. The electron beam passed through a tungsten radiator (186 mg/cm<sup>2</sup> thickness) about 5 cm upstream from the  $^{13}\text{C}$  target, and the mixed photon-electron beam then passed through the target. The target used was a self-supporting disc of pressed  $^{13}\text{C}$  powder (99% isotopically pure  $^{13}\text{C}$ ). Pions emerging from the target at  $90^\circ$  were momentum analyzed in a magnetic spectrometer system which has been previously described in detail<sup>14</sup> (see Table I for parameters), and were detected in a multiwire proportional counter mounted in the focal plane. For particle identification, a series of three scintillation counters and one Čerenkov veto counter was placed behind the wire chamber. Data were stored on an event-by-event basis. Information recorded with each event included chamber wire firings, scintillator and Čerenkov pulse heights, and relative pulse times.

## III. DATA REDUCTION AND ANALYSIS

Data reduction and analysis procedures have been described in detail elsewhere.<sup>14,15</sup> Event-by-event records were first sorted to separate background from real events. The wire chamber spectrum of acceptable pion events was corrected for channel-by-channel efficiency variations; these corrections were obtained experimentally by measuring the smooth spectrum obtained at an electron energy of 230 MeV with the same spectrometer setting. Dead time corrections ( $\approx 15\%$ ) were made, and the wire

TABLE I. Spectrometer parameters.

Radius of curvature	41.7 cm
Solid angle	15 msr
Dynamic range, $\Delta p/p$	14%
Intrinsic momentum resolution	$7 \times 10^{-3}$

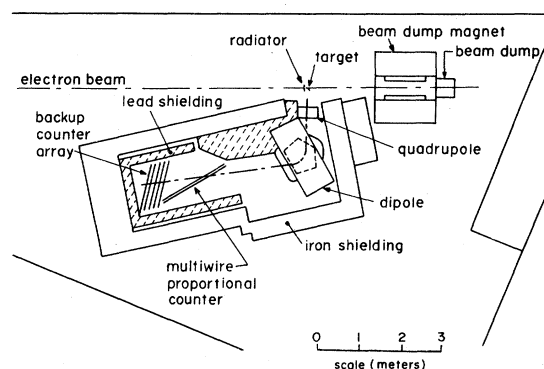


FIG. 2. Experimental layout.

chamber spectra taken at various electron energies at a particular spectrometer setting were then combined into a plot of the number of pions per unit energy versus electron energy for a particular pion kinetic energy range (isochromat plot). Finally each isochromat was fitted by a combined real and virtual photon spectrum to determine cross sections. The plot for  $T_\pi \approx 42$  MeV is given in Fig. 3.

The spectrum shape used to describe real photons

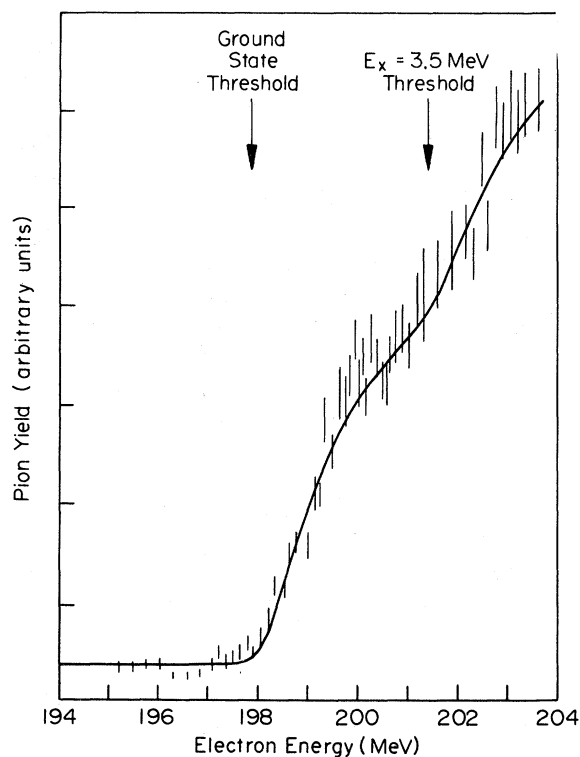


FIG. 3. Experimental isochromat (relative number of pions per MeV versus electron energy) obtained at 42 MeV pion energy. The solid curve is the fit to the data as described in the text, and includes contributions from background and the transitions to the ground state and 3.5 MeV region.

TABLE II. Experimental results for  $^{13}\text{C}(\gamma, \pi^+)$ . Errors quoted are statistical only (see text).

$T_\pi$ (MeV)	$q_{\text{lab}}$ ( $\text{fm}^{-1}$ )	$d\sigma/d\Omega$ ( $90^\circ$ lab)	
		$E_x=0$	$E_x=3.5$ MeV
18	0.94	$178 \pm 9$ nb/sr	
29	1.03	$230 \pm 4$	
42	1.15	$325 \pm 10$	$166 \pm 18$

from bremsstrahlung in the radiator and target was calculated using a code of Matthews and Owens.<sup>16</sup> The electroproduction was described in terms of a spectrum of virtual photons which were assumed to give rise to the same  $(\gamma, \pi)$  cross section as real photons of the same energy. The virtual photon spectrum was obtained from an expression of Dalitz and Yennie,<sup>17</sup> multiplied by an experimentally-determined correction factor of 1.25.<sup>18</sup> Calculations of these spectra took account of electron and pion energy losses in the radiator and target, and system energy resolution. The real and virtual spectra were then added to give an overall photon spectrum describing the combined effect of photoproduction and electroproduction. Figure 3 shows a fit of this combined spectrum to the data at  $T_\pi \simeq 42$  MeV. Real bremsstrahlung photons contributed about two-thirds of the pion yield in the present experiment and virtual photons about one-third.

In order to fix the absolute cross section scale, hydrogen normalization runs were made for each of the three pion energies using a  $54 \text{ mg/cm}^2$  polyethylene target. The pion yield from hydrogen dominates in these runs; similar runs were made with a graphite target to permit subtraction of the carbon contribution to the yield. Statistics for the net hydrogen yield were typically 4%. Absolute cross section values for  $^1\text{H}(\gamma, \pi^+)$  were obtained from the tabulation of Genzel *et al.*<sup>19</sup> for that reaction.

#### IV. RESULTS AND DISCUSSION

Differential cross section values obtained from the experiment for transitions to the ground state and 3.5 MeV region of  $^{13}\text{B}$  at  $90^\circ$  (lab) are given in Table II. The errors quoted are statistical only. There are several important sources of systematic errors. Among these are the following, with their estimated contribution to the overall systematic error: variation in the  $(\gamma, \pi)$  cross section over the system acceptance energy range (2%); and uncertainties in target thickness (5%), in real and virtual photon spectra (8%), in corrections for pion decay (4%), in normalization target thickness (5%), and in

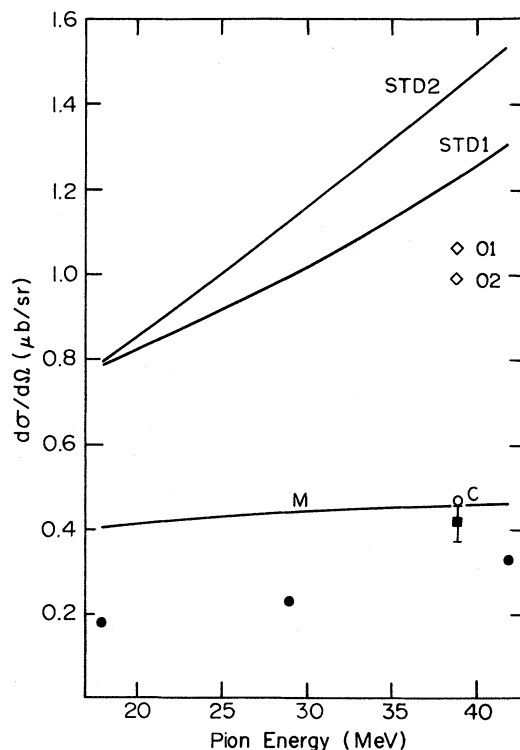


FIG. 4. The solid circles are the present experimental results. The solid square experimental point is due to Shoda *et al.* (Ref. 13). The remaining curves and points are the results of several DWIA calculations. The curve labeled M is the result of a calculation by Maleki (Ref. 20), the point labeled C is Cheon's calculation (Ref. 21), and the curves labeled STD1 and STD2 are the results of the calculation of Singham, Tabakin, and Dytman (Ref. 23) using the 1979 and 1982 pion optical potentials of Stricker *et al.*, respectively. The open diamond points labeled O1 and O2 are due to Sato, Koshigiri, and Ohtsubo (Ref. 22), using Hauge-Maripuu (HM) and Cohen-Kurath (CK) wave functions, respectively.

the published  $\text{H}(\gamma, \pi^+)$  cross section values<sup>19</sup> used for normalization (10%). We assume these contributions are independent and add in quadrature, giving an overall systematic error of about 16%. Figures 4 and 5 show the present results as well as the  $90^\circ$  point of Shoda *et al.*<sup>13</sup> The latter is higher than the present data, but the two results agree within their combined systematic errors.

Four independent DWIA calculations have been made by Maleki (M),<sup>20</sup> Cheon (C),<sup>21</sup> Sato, Koshigiri, and Ohtsubo (O),<sup>22</sup> and Singham, Tabakin, and Dytman (STD).<sup>23</sup> The results of these calculations are shown in Fig. 4. All of them include both Coulomb and strong interaction distortions of the pion in the final state, and represent the strong interaction effects by an optical potential. The M and

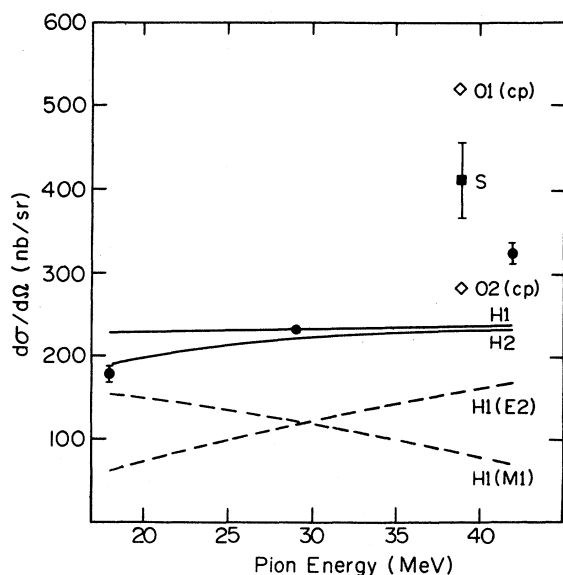


FIG. 5. The solid circles are the present experimental results and the solid square is the  $90^\circ$  result of Shoda *et al.* (Ref. 13). Error bars denote statistical errors only (see text). The curves labeled H1 and H2 are the results of Helm model calculations using the code of Nagl and Überall (Ref. 31) and the parameters of Table III. The points labeled O1(cp) and O2(cp) are as calculated by Sato, Koshigiri, and Ohtsubo (Ref. 22) using HM and CK wave functions, respectively as in Fig. 4, but now including core polarization effects.

C calculations use similar inputs and yield similar results. They use the full elementary photoproduction amplitude of Chew, Goldberger, Low, and Nambu (CGLN),<sup>24</sup> the intermediate coupling nuclear wave functions of Cohen and Kurath (CK),<sup>25</sup> and a local Laplacian optical potential to represent the pion-nucleus final state interaction. The calculation of Sato, Koshigiri, and Ohtsubo also uses the CGLN amplitude and the CK wave functions, as well as wave functions due to Hauge and Maripuu (HM).<sup>26</sup> They employ the pion optical potential of Stricker *et al.*<sup>27</sup> Singham, Tabakin, and Dytman use the Blomqvist-Laget amplitude,<sup>28</sup> CK wave functions, and both the 1979 and 1982 versions of the pion optical potential of Stricker *et al.*<sup>27,29</sup> (STD1 and STD2, respectively). The newer version gives a better fit to pionic atom and pion scattering data. As seen in Fig. 4, the results of these calculations fall into two groups. One group comprises STD and O and the other M and C, with the STD and O results  $\approx 2$  times higher than those of M and C. It does not appear reasonable to attribute this clear discrepancy to the differences in treating pion distortion; these are only expected to yield  $\sim 20\%$  effects.<sup>30</sup>

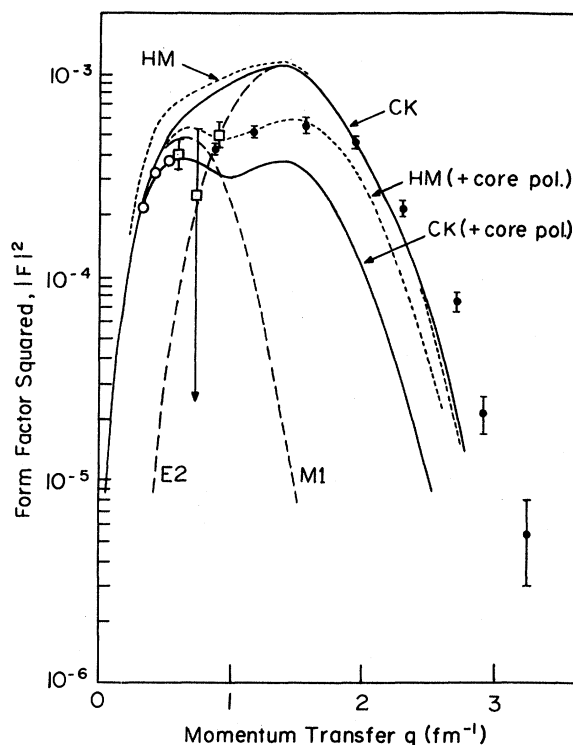


FIG. 6. Experimental results for the form factor squared ( $|F|^2$ ) as obtained from  $^{13}\text{C}(e,e')$  ( $E_x=15.11$  MeV) (open circles: Ref. 9; open squares: Ref. 10; solid circles: Ref. 11) are shown along with  $|F|^2$  calculated (Ref. 22) using Cohen-Kurath wave functions (solid curves) and Hauge-Maripuu wave functions (dotted curves) with and without core polarization corrections.

The wave functions used in these DWIA calculations have been tested<sup>20-23</sup> against inelastic electron scattering data.<sup>9-11</sup> Figure 6 compares the calculated transverse form factor squared ( $|F|^2$ ) to the  $(e,e')$  experimental results. Over the range of momentum transfer  $q$  appropriate to the present  $(\gamma,\pi)$  experiment ( $q$  between  $0.94$  and  $1.15$   $\text{fm}^{-1}$ ), both CK and HM wave functions yield  $|F|^2$  values significantly higher than experiment. For example, the CK  $|F|^2$  is higher than experiment by a factor of about 2.0 over this range of momentum transfer.

Sato, Koshigiri, and Ohtsubo have also included core polarization effects in their calculations using both the CK and HM wave functions [O1(cp) and O2(cp), respectively]. Their  $(\gamma,\pi)$  results are shown in Fig. 5 and their form factor results in Fig. 6. In both cases, inclusion of core polarization has a very significant effect, causing a reduction by a factor  $\approx 2$  and bringing the calculated values down into closer agreement with experiment.

Also shown in Fig. 5 are the results of Helm model (H) calculations using a code due to Nagl and

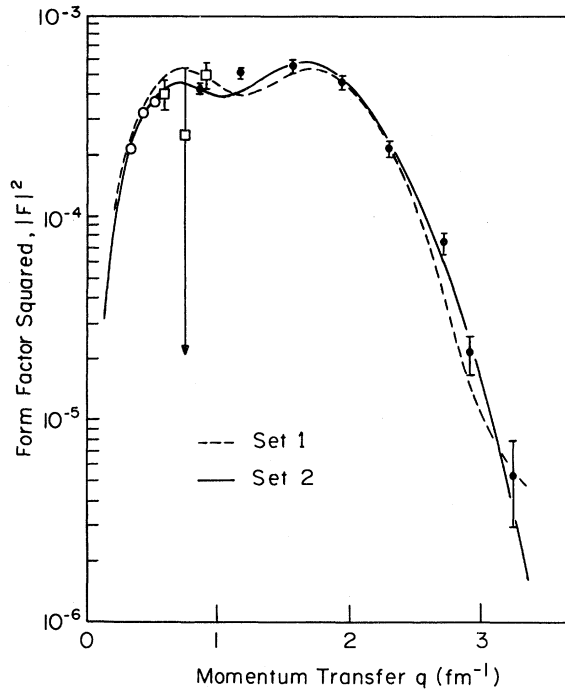


FIG. 7. The form factor squared  $|F|^2$  versus momentum transfer for  $^{13}\text{C}(e,e')$  ( $E_x = 15.11$  MeV). The experimental data are as in Fig. 6. The curves are Helm model fits as described in the caption to Table III.

Überall.<sup>3</sup> In these calculations the nuclear structure information is parametrized from electron scattering data using the Helm model. The elementary photoproduction amplitude of Berends *et al.*<sup>32</sup> and a second-order pion optical potential are used. Two curves are shown in Fig. 5 corresponding to two sets of Helm parameters which fit the  $(e,e')$  form factor data (Fig. 7) reasonably well. The parameters used are given in Table III.

We next compare the results of these  $(\gamma,\pi)$  calculations to experiment (Figs. 4 and 5). At  $T_\pi = 18$  and 29 MeV, the Helm model calculations (H1, H2) fit experiment quite well. However, both the M and STD results are higher than experiment, by factors of about 2 and 4, respectively. Since the CK  $|F|^2$  also exceeds experiment by a factor  $\simeq 2$ , this suggests that the discrepancy between the STD and M calculations and experiment for  $(\gamma,\pi)$  at these energies is attributable at least in part to the shortcomings of the CK nuclear wave functions used.

At  $T_\pi$  near 40 MeV, the situation is more complicated. The factor of 2 discrepancy between the M and H calculations is still present at this energy, but H1 and H2 are now lower than experiment, and M is significantly closer to experiment than at lower energies. The STD results still exceed the data by a factor  $\simeq 4$ , but unlike H and M they do

TABLE III. Helm parameters for form factor fits shown in Fig. 6. The parameters are as defined in Ref. 39, for example. The  $R(M1)$  values for both sets and  $\gamma_{LL+1}$  for set 1 are taken equal to the values of Ref. 39 for  $^{12}\text{C}(M1)$  at 15.1 MeV. The strength parameters are constrained to be consistent with the experimental photon width for the transition. In set 1 the parameters are determined by fitting the  $M1$  form factor to the five lowest  $q$  points and then fitting  $E2$  to the difference between the  $M1$  calculation and experiment. In set 2 the  $E2$  form factor is first fit to the seven highest  $q$  points and then  $M1$  is fit to the difference between  $E2$  and experiment.

	Set 1		Set 2	
	$M1$	$E2$	$M1$	$E2$
$R = \bar{R}$	2.24 fm	1.60 fm	2.24 fm	1.45 fm
$g = \bar{g}$	0.65 fm	0.79 fm	0.86 fm	0.85 fm
$\beta_L$		0.532		0.650
$\gamma_{LL}$		0.916		1.219
$\gamma_{LL-1}$	0.611		0.611	
$\gamma_{LL+1}$	0		-0.060	

well reproduce the experimental energy dependence. The O1 and O2 results without core polarization are a factor of  $\simeq 3$  higher than experiment (Fig. 4); with core polarization included, they bracket experiment (Fig. 5). A comparison of these calculations with the angular distribution data of Shoda *et al.*<sup>13</sup> taken near 40 MeV shows that the calculations of Sato *et al.* (including core polarization) all fit that data reasonably well at all angles. The latter calculation, however, appears to be favored over the other calculations which do not include core polarization effects in that it achieves fair agreement with both the  $(\gamma,\pi)$  cross sections and  $(e,e')$  form factor data.

We do not understand why the situation is more confused near 40 MeV than at 18 MeV. It may be significant that both the  $(\gamma,\pi)$  cross section and  $|F|^2$  for this  $M1$ - $E2$  transition are dominated by the  $M1$  component at 18 MeV but by the  $E2$  component at 40 MeV.

The closely-related measurement of Martoff *et al.*<sup>33</sup> on  $^{13}\text{C}(\pi^-, \gamma)^{13}\text{B}(\text{g.s.})$  connects the same states as the present  $(\gamma,\pi)$  work but at lower  $q$  ( $\sim 0.7$  fm $^{-1}$ ). Their measured value for the branching ratio is  $6.0 \pm 1.2 \times 10^{-4}$ , while the theoretical value of Dogotar *et al.*<sup>34</sup> using CK wave functions without core polarization corrections is  $8.8 \times 10^{-4}$ . Experiment and theory are somewhat closer than are the present experiment and the theoretical value of M at  $T_\pi = 18$  MeV. However, the  $(\pi^-, \gamma)$  result is at lower  $q$ , where the CK  $(e,e')$  form factor is closer to experiment (Fig. 6). In fact, the ratio of

theoretical to experimental values for  $(\pi^-, \gamma)$  approximately reflects the corresponding form factor ratio.

One additional remark may be made about the  $E2$  part of this transition. As pointed out by Flanz *et al.*,<sup>35</sup> the convective current part of the transverse  $E2$  form factor identically vanishes for a pure  $1p$  shell configuration in a harmonic oscillator basis, leaving only the magnetization current part. Since the  $(\gamma, \pi)$  process is expected to involve mostly spin-flip transitions for  $T_\pi < 50$  MeV, as in the present experiment, we would expect in this case that the Helm model should do a good job of using the form factor data to predict the  $(\gamma, \pi)$  cross sections.

In summary, the overall comparison between theory and experiment for  $^{13}\text{C}(\gamma, \pi^+)^{13}\text{B}(\text{g.s.})$  is in an unsatisfactory state. Moreover, the discrepancies among the several calculations are larger than is reasonable on the basis of the differences in their inputs. Further work is needed to resolve these discrepancies and to assess the importance of core polarization effects.

We also observe significant strength at 3.5 MeV excitation in  $^{13}\text{B}$  at  $T_\pi = 42$  MeV (Table II). Strength near this excitation energy is also seen in  $^{13}\text{C}(\pi^-, \gamma)$  (Ref. 33) and in  $^{13}\text{C}(\gamma, \pi^+)$  studies at

Tohoku University.<sup>36</sup> Calculations of Eramzhyan *et al.*<sup>37</sup> place significant  $M2$  strength at this energy. The first four excited states of  $^{13}\text{B}$  are clustered near 3.5 MeV (see Fig. 1) and cannot be resolved in the present experiment. Two of them, those at 3.48 and 3.68 MeV, are reported<sup>38</sup> to be positive parity states with spins of  $\frac{1}{2}$ ,  $\frac{3}{2}$ , or  $\frac{5}{2}$ , and are possible candidates to carry  $M2$  strength.

#### ACKNOWLEDGMENTS

This work was supported by National Science Foundation Grants PHY77-09408 and PHY80-06954, by the Department of Energy through Contract EY-76-C-02-3069, and by the U.S.-Japan Cooperative Science Program. Two of us (K.S. and M.Y.) were supported by a grant from the Japan Society for the Promotion of Science under this latter program. We thank the staff of the Bates Linear Accelerator for their assistance and support in carrying out the experimental work, and B. N. Sung for assisting us with the data taking. We thank A. Nagl and H. Überall for allowing us to use their Helm model code, and S. Maleki, I.-T. Cheon, and H. Ohtsubo for providing us with their theoretical results prior to publication.

\*Present address: Department of Physics, Louisiana State University, Baton Rouge, Louisiana 70803.

†Present address: Lawrence Livermore National Laboratory, Livermore, California 94550.

‡On leave from University of Saskatchewan, Saskatoon, Saskatchewan, Canada.

§Present address: Department of Physics, Carnegie-Mellon University, Pittsburgh, Pennsylvania 15213.

||Present address: General Research Corporation, 7655 Old Springhouse Road, Westgate Research Park, McLean, Virginia 22102.

<sup>1</sup>K. Shoda, H. Ohashi, and K. Nakahara, Phys. Rev. Lett. **39**, 1131 (1977); Nucl. Phys. **A350**, 377 (1980).

<sup>2</sup>N. Paras *et al.*, Phys. Rev. Lett. **42**, 1455 (1979).

<sup>3</sup>K. Min *et al.*, Phys. Rev. Lett. **44**, 1384 (1980).

<sup>4</sup>D. Rowley *et al.*, Phys. Rev. C **25**, 2652 (1982).

<sup>5</sup>M. Yamazaki, Ph.D. thesis, Tohoku University, 1981 (unpublished).

<sup>6</sup>H. Ohashi *et al.*, *Photopion Nuclear Physics*, edited by P. Stoler (Plenum, New York, 1979), pp. 193–198.

<sup>7</sup>P.-K. Teng *et al.*, Phys. Rev. C **26**, 1313 (1982).

<sup>8</sup>K. Shoda, O. Sasaki, and T. Kohmura, Phys. Lett. **101B**, 124 (1981).

<sup>9</sup>G. Wittwer, H.-G. Clerc, and G. A. Beer, Phys. Lett. **30B**, 634 (1969).

<sup>10</sup>C. S. Yang *et al.*, Nucl. Phys. **A162**, 71 (1971).

<sup>11</sup>R. S. Hicks *et al.* (private communication).

<sup>12</sup>J. LeRose *et al.*, Phys. Rev. C **25**, 1702 (1982).

<sup>13</sup>K. Shoda *et al.*, in *Proceedings of the Ninth International Conference on High Energy Physics and Nuclear Structure, Versailles, 1981*, edited by P. Catillon, P. Radvanyi, and M. Porneuf (North-Holland, Amsterdam, 1982).

<sup>14</sup>N. Paras *et al.*, Nucl. Instrum. Methods **167**, 215 (1979).

<sup>15</sup>J. LeRose, Ph.D. thesis, Rensselaer Polytechnic Institute, 1981 (unpublished); P. Stoler *et al.* (unpublished).

<sup>16</sup>J. L. Matthews and R. O. Owens, Nucl. Instrum. Methods **111**, 157 (1973).

<sup>17</sup>R. H. Dalitz and D. R. Yennie, Phys. Rev. **105**, 1598 (1957).

<sup>18</sup>P. Stoler *et al.*, Phys. Rev. C **22**, 911 (1980).

<sup>19</sup>H. Genzel and W. Pfeil, *Landolt-Börnstein: Zahlenwerte und Funktionen aus Naturwissenschaften und Technik*, Neue Serie, edited by H. Schopper (Springer, Berlin, 1973), Vol. 8.

<sup>20</sup>S. Maleki, Ph.D. thesis, Rensselaer Polytechnic Institute, 1981 (unpublished).

<sup>21</sup>I.-T. Cheon (private communication).

<sup>22</sup>T. Sato, K. Koshigiri, and H. Ohtsubo (unpublished).

<sup>23</sup>M. Singham, F. Tabakin, and S. Dytman (private communication).

- <sup>24</sup>G. F. Chew, M. L. Goldberger, F. E. Low, and Y. Nambu, *Phys. Rev.* **106**, 1345 (1957).
- <sup>25</sup>S. Cohen and D. Kurath, *Nucl. Phys.* **73**, 1 (1965).
- <sup>26</sup>P. S. Hauge and S. Maripuu, *Phys. Rev. C* **8**, 1609 (1973).
- <sup>27</sup>K. Stricker, H. McManus, and J. A. Carr, *Phys. Rev. C* **19**, 929 (1979).
- <sup>28</sup>I. Blomqvist and J. M. Laget, *Nucl. Phys.* **A280**, 405 (1977).
- <sup>29</sup>J. A. Carr, H. McManus, and K. Stricker-Bauer, *Phys. Rev. C* **25**, 952 (1982).
- <sup>30</sup>W. C. Haxton, *Phys. Lett.* **92B**, 37 (1980).
- <sup>31</sup>A. Nagl and H. Überall (private communication).
- <sup>32</sup>F. A. Berends, A. Donnachie, and D. L. Weaver, *Nucl. Phys.* **B4**, 1 (1967).
- <sup>33</sup>C. J. Martoff *et al.*, in Proceedings of the Workshop on Nuclear Structure with Intermediate Energy Probes, Los Alamos, New Mexico, 1980, Los Alamos Scientific Laboratory Report No. LA 8303-C, 1980, pp. 336–351.
- <sup>34</sup>G. E. Dogotar *et al.*, quoted in Ref. 33.
- <sup>35</sup>J. B. Flanz *et al.*, *Phys. Rev. Lett.* **41**, 1642 (1978).
- <sup>36</sup>K. Min *et al.*, in *Proceedings of the Ninth International Conference on High Energy Physics and Nuclear Structure, Versailles, 1981*, edited by P. Catillon, P. Radvanyi, and M. Porneuf (North-Holland, Amsterdam, 1982).
- <sup>37</sup>R. A. Eramzhyan, M. Gmitro, and H. R. Kissener, *Nucl. Phys.* **A338**, 436 (1980).
- <sup>38</sup>F. Ajzenberg-Selove, *Nucl. Phys.* **A360**, 1 (1981).
- <sup>39</sup>H. Überall, B. A. Lamers, J. B. Langworthy, and F. J. Kelly, *Phys. Rev. C* **6**, 1911 (1972).